





A decoupling strategy for protecting sensitive process information in cooperative optimization of power flow

Tim Varelmann¹  | Joannah I. Otashu^{2,3} | Kyeongjun Seo² | Adrian W. Lipow¹  | Alexander Mitsos^{1,4,5}  | Michael Baldea^{2,6} 

¹Process Systems Engineering (AVT.SVT), RWTH Aachen University, Aachen, Germany

²McKetta Department of Chemical Engineering, The University of Texas at Austin, Austin, Texas, USA

³Process Systems Enterprise, Houston, TX, USA

⁴JARA-CSD, Aachen, Germany

⁵Institute of Energy and Climate Research, Energy Systems Engineering (IEK-10), Forschungszentrum Jülich GmbH, Jülich, Germany

⁶Oden Institute for Computational Engineering and Sciences, The University of Texas at Austin, Austin, TX, USA

Correspondence

Michael Baldea, McKetta Department of Chemical Engineering, The University of Texas at Austin, Austin, TX 78712, USA.
Email: mbaldea@che.utexas.edu

Funding information

Deutsche Forschungsgemeinschaft (IRTG Modern Inverse Problems), Grant/Award Number: 33849990/GRK2379; National Science Foundation CAREER Award, Grant/Award Number: 1454433

Abstract

Optimal power flow (OPF) with close cooperation between the power grid and flexible electricity-intensive chemical processes can reduce costs for the grid and for electricity users. However, this would require sharing detailed chemical process models, which may reveal confidential information and potentially jeopardize competitive advantages for a chemical process operator. We propose an algorithm that enables economically advantageous cooperation without the need to exchange sensitive information. Low-order linear models are used to represent the dynamic behavior of electricity-intensive processes. We integrate these models into the OPF problem and solve the problem using a decoupling strategy based on Benders-type cuts. The cuts introduce limited communication between the chemical processes and the grid without exchanging explicit information pertaining to the process dynamics and performance. Our results reproduce solutions obtained by sharing detailed process models up to a user-defined optimality gap for several test cases that reflect both normal and congested grid states. We also investigate the trade-off between the value of the optimality gap and computational effort. Finally, we study the scaling behavior of the iterative procedure with respect to flexible loads at multiple grid locations.

KEYWORDS

congestion management, cooperative optimal power flow, demand-side management, load modeling

1 | INTRODUCTION

Solar and wind power plants are becoming major producers of electricity worldwide. Also, electricity-intensive industries have become hybrid consumers and suppliers of their on-site generation capacities. Renewable energy sources bring formerly unknown challenges for the operation of electricity grids. Originating from natural sources of energy, the power production of solar and wind energy plants is difficult to predict and highly variable over short time scales. Aiming for

stable and safe grid operation, two branches of research have emerged recently: smart grid technology focuses on optimal load distribution in networks over time and space,^{1,2} whereas demand side management (DSM) is an effort to monetize the operational flexibility of loads to shape demand curves.^{3,4,5}

Both fields have received considerable research attention in the past years.^{6,7} As a result, different pricing schemes such as peak pricing, other forms of time-of-use contracts, day-ahead pricing, or base-load contracts are offered to large localized energy consumers.

This is an open access article under the terms of the Creative Commons Attribution License, which permits use, distribution and reproduction in any medium, provided the original work is properly cited.

© 2021 The Authors. *AIChE Journal* published by Wiley Periodicals LLC on behalf of American Institute of Chemical Engineers.

Nevertheless, when grid operators act and decide separately from users, they cannot utilize the full potential of DSM in electrical power grids. In a recent article, Otashu et al. have examined the effect of cooperative optimal power flow (OPF) calculations, in which grid operators are granted unrestricted access to the full operational flexibility of large industrial energy consumers to optimize the electrical energy transmission.⁸ We will refer to this problem as *integrated formulation* of cooperative OPF problems. This results in cost improvements similar to conventional demand response (DR) for both grid transmission and process operation in normal grid conditions. In congested grids, cooperative OPF can reduce grid transmission cost and electricity prices more effectively than conventional DR, and can prevent load shedding. This makes the cooperative optimization approach superior, in particular in congested conditions, for example, after a critical failure of a transmission line or a generator. However, the cooperative approach with the integrated formulation hinges on process operators sharing confidential information via detailed process models. Hence, industry would likely be reluctant to support such concepts. A more acceptable solution would be to allow grid operators to control some of the degrees of freedom in the chemical plant without sharing detailed models with confidential information. Motivated by the above, the key contributions of this article are:

- A decoupling strategy tailored to ensure confidentiality in cooperative OPF problems while staying close to the integrated solution.
- A case study of the decomposition approach, where we benchmark its results against the integrated solution.

2 | MOTIVATION FOR DECOUPLING COOPERATIVE OPF PROBLEMS

2.1 | Conventional OPF with DR and their limitations

An important part of managing the power grid involves balancing power generation and demand across the power network in real time. Power supply from various generating sources and storage devices is constantly being modulated to match the variable power demand and, in recent times, to also balance fluctuations arising from renewable power generation units. Power generation target levels can be computed by solving the *conventional OPF problem* of the general form (1).^{9,10,11}

$$\min_{\mathbf{p}^{\text{gen}}, \mathbf{T}, \boldsymbol{\theta}} \sum_{i \in \Omega_{\text{Bus}}} \sum_{t=1}^H F_i(\mathbf{p}_{i,t}^{\text{gen}}) \quad (1a)$$

s.t.

$$\mathbf{p}_{i,t}^{\text{gen}} - \mathbf{p}_{i,t}^{\text{load}} = \sum_{j \in \Omega_i^j} T_{(i,j),t}, \quad \forall i \in \Omega_{\text{Bus}} \quad (1b)$$

$$T_{(i,j),t} = \beta \cdot S_{ij}(\theta_{j,t} - \theta_{i,t}), \quad \forall (i,j) \in \Omega_l \quad (1c)$$

$$T_{(i,j)}^{\min} \leq T_{(i,j),t} \leq T_{(i,j)}^{\max}, \quad \forall (i,j) \in \Omega_l \quad (1d)$$

$$\theta_i^{\min} \leq \theta_{i,t} \leq \theta_i^{\max}, \quad \forall i \in \Omega_{\text{Bus}} \setminus \{\text{slackbus}\} \quad (1e)$$

$$\theta_{\text{slackbus},t} = 0 \quad (1f)$$

$$\mathbf{p}_{i,t}^{\text{gen},\min} \leq \mathbf{p}_{i,t}^{\text{gen}} \leq \mathbf{p}_{i,t}^{\text{gen},\max} \quad (1g)$$

$$\mathbf{p}_{i,t}^{\text{gen}} - \mathbf{p}_{i,t-1}^{\text{gen}} \leq \mathbf{p}_{i,t}^{\text{gen},\text{rampup}} \cdot \Delta t \quad (1h)$$

$$\mathbf{p}_{i,t}^{\text{gen}} - \mathbf{p}_{i,t-1}^{\text{gen}} \geq -\mathbf{p}_{i,t}^{\text{gen},\text{rampdown}} \cdot \Delta t \quad (1i)$$

where all constraints (1b)–(1i) have to hold for the entire time horizon under consideration, that is, $\forall t \in \{1, \dots, H\}$. Here, we will assume a 15-min-interval discretization of 1 day, so $H = 96$. We use i as index over the set of buses Ω_{Bus} . Ω_i^j is the set of buses connected to bus i via a transmission line, Ω_l is the set of transmission lines, and t denotes a time slot of duration Δt . The decision variables are the generator target levels of all generators in the grid, $\mathbf{p}_t^{\text{gen}} \in \mathbb{R}^{H \times |\Omega_{\text{Bus}}|}$; the power flow between connected pairs of buses i and j , $\mathbf{T} \in \mathbb{R}^{H \times |\Omega_l|}$; and the bus angles w.r.t. the slack bus in radians, $\boldsymbol{\theta} \in \mathbb{R}^{H \times |\Omega_{\text{Bus}}|}$. The $F_i(\cdot)$ are operating cost functions of the generators, whose sum is minimized with the objective (1a). Each $\mathbf{p}_{i,t}^{\text{load}}$ is the power demand on a bus denoted with i in time slot t . S is the circuit susceptance matrix with entries S_{ij} in pu (per unit on a base $\beta = 100$ MW). The marginal values of the nodal power balances (1b) provide the nodal electricity prices.

Problem (1) is a linear program (when using linear generator cost functions). Its solution is the direct-current (DC) OPF that approximates the more complex alternating current (AC) power flow problem.¹⁰ In transmission systems that have a diverse set of voltage magnitudes or where (1e) cannot be fulfilled, the AC formulation is required to get accurate solutions.¹¹

In the OPF problem (1), the power demand at each bus, $\mathbf{p}_{i,t}^{\text{load}}$, is a fixed load level metered in real-time from power consumption sites or estimated using historical power demand. When industrial electricity users participate in DR programs, they exploit the electricity price profiles that are computed assuming that the values for $\mathbf{p}_{i,t}^{\text{load}}$ are known and will not change over the time horizon considered. However, in response to the electricity price profiles, industrial participants may schedule their power demand in a way that differs from the values assumed for $\mathbf{p}_{i,t}^{\text{load}}$ in problem (1). This violates the assumption that lead to the electricity price profiles. Consequently, DR activities can create undesired effects on electricity grids such as rebound peaks¹² or even additional transmission congestion.¹³ As visualized in Figure 1, any sequence of solving OPF problems and DRs separately leads to a mismatch between real industrial demand and demand assumed by the OPF problem. An iterative approach to finding a market equilibrium for price profiles and demand profiles is not guaranteed to converge and requires heuristic stopping criteria,¹⁴ or hard-to-derive demand-price sensitivity matrices.¹⁵

The *cooperative OPF problem*, developed in our previous work,⁸ avoids sequencing by integrating the conventional OPF problem and the scheduling of industrial demand into a monolithic optimization problem in the integrated formulation. The demand of cooperating electricity users becomes a decision variable of the monolithic

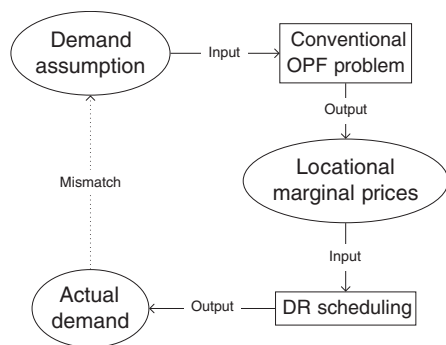


FIGURE 1 Conventional optimal power flow (OPF) problems assume an industrial demand based on historical data. The OPF solution provides electricity prices which can be exploited by demand-responsive end-users. The cost-optimal demand profile for the end-user is heavily influenced by the locational marginal prices and will likely not match the original assumption made to formulate the OPF problem. This mismatch can lead to undesired effects such as rebound peaks or an induced grid congestion

problem and can thus be incorporated both in the grid description as load and in the process model describing end-user behavior. As a consequence, the cooperative OPF problem eliminates the mismatch between modeled and implemented process demand. Our previous results show⁸ that the cooperative and the sequential approach are economically comparable in normal grid conditions. However, the cooperative approach can be superior to the sequential approach in congested grids because it can avoid load shedding and reduce congestion. This can improve the economics of the grid and the resulting electricity prices tremendously.⁸ Note that transmission constraints such as (1d) are active per definition in congested grids. Our previous results⁸ support the interpretation that the mismatch between assumed and implemented process demand visualized in Figure 1 that is present in the sequential approach is a drawback with significant economical impact in congested grids.

2.2 | Cooperative OPF and its limitations

Our previous work⁸ introduced the cooperative OPF approach. To make this article more self-contained, we highlight the differences between cooperative OPF problems and conventional OPF problems in this section. We also state limitations of the previously proposed integrated cooperative OPF formulation, one of which will motivate this article. For more details on the cooperative OPF approach, we refer the reader to our previous work.⁸

We represent the power consumption levels of demand responsive end-users with simple dynamic models where end-user demand is modeled as an optimization variable. Then, we formulate the integrated problem: an optimization problem comprising all grid-related decisions and constraints, including the dynamic models of all cooperating plants. By integrating the two components of the cooperative OPF approach, we recognize that we renounce the end-user's ability to minimize their own electricity cost. In this formulation, we

can allocate the flexible demand of cooperating end-users toward minimizing generation and transmission cost directly, together with other grid-related decisions. In contrast, flexible user demand only reacts to a price profile in conventional OPF formulations. As shown in our previous work,⁸ cooperative OPF solutions can be superior to conventional OPF solutions that are applied in conjunction with (independent, user-level) “downstream” DR activities.

In its current state of development, the cooperative OPF approach exhibits two major limitations. First, the operational flexibility of cooperating end-users is used to minimize the overall generation and transmission cost of the grid. While this is desirable from a grid perspective, there is no guarantee that the cost reductions achieved through the cooperation of end-users and grid influence the locational marginal prices of the buses on which the cooperating end-users are connected to the grid. In particular, it is possible that some demand-responsive end-users would have lower electricity costs (based on locational marginal prices) if they denied the cooperation in order to exploit the locational marginal prices on their bus for their own benefit only. Despite the lack of guaranteed cost reduction through cooperation, several cases studied in our previous work⁸ led to lower electricity cost for the end-users than they would have had without cooperation. Also, we assume that the cooperating industrial process only focuses on reducing electricity cost. One could think of other relevant types of operating cost, for example, cooling or heating cost. With our current framework, reducing these costs may not be addressed properly. In order to align all end-users' monetary interests with the goal of globally minimizing generation and transmission cost and also considering more general process costs, some cooperation-compensation mechanism is needed that guarantees cooperating end-users lower operating costs than they could achieve through local exploitation of electricity prices. However, such a compensation mechanism is out of the scope of this article.

The second limitation of cooperative OPF problems will be addressed in this article. In order to formulate the integrated cooperative OPF problem, demand-responsive end-users have to provide models describing the dynamic behavior of the process and all constraints related to safety, quality, and product demand to the grid operators. This requirement poses a major confidentiality problem for operators of chemical plants, which we aim to mitigate with this article.

2.3 | Decoupling cooperative OPF and limiting information exchange

A cooperation between grid and demand-responsive end-user should find a demand profile that contributes to minimal generation and transmission cost for the grid but also allows feasible operation of the cooperating industrial process. In this article, we show that we can achieve this goal without explicitly sharing a detailed process model. In particular, our purpose is to avoid sharing explicitly a set of operationally relevant variables, such as product demand, quality constraints, process capacities, storage capacities, and safety constraints. Of course, these variables influence which demand profiles are feasible and which are not. However, the grid operators are not interested

in the underlying reasons for feasibility of demand profiles. Therefore, it is possible to project all process variables onto the space of power demand profiles, which can then be shared with the grid.

In light of the above, we provide an outer approximation of the feasible region of power profiles to the grid that can be incorporated in the OPF problem to shape the power demand of cooperating loads to minimize generation and transmission costs. To ensure the feasibility of the power demand profile, we iteratively refine this outer approximation. We demonstrate that the refining process converges to an optimal solution of the integrated problem, leading to an optimal cooperative OPF solution without sharing explicit process details. While some literature sources claim that the space of power profiles already reveals substantial proprietary information when published,^{16,17} our experience indicates that it is nearly impossible to reconstruct accurate production characteristics in multiproduct plants only from power profiles.

3 | LITERATURE REVIEW

Protecting confidential information is an important topic in many contexts, which leads to a variety of techniques. For power networks, Anderson et al. showed that publication of aggregated data sets maintains confidentiality for utility companies.¹⁸ This would only allow cooperation of large conglomerations of processes located on the same bus, which is too restrictive for our purposes. Another concept to obfuscate information is differential privacy¹⁹ with noise added to queries. The added noise poses a major theoretical challenge to guarantee convergence of any solution method to an optimum. Recently, methods to introduce differential privacy of loads in OPF benchmark problems were presented in References 16 and 17. The true loads are obfuscated in a way that minimizes the influence of the added noise on the OPF solution. However, cooperative OPF computations have to inherently ensure confidentiality, rather than adding this feature in a postprocessing stage.

Since DSM allows to reduce electricity cost for energy-intensive processes and has beneficial effects on grid stability, the field got a lot of research attention recently. The first and most broadly studied DSM application process is air separation.^{20,21,22} Furthermore, DSM approaches were developed for steel production,²³ combined heat and power plants,²⁴ metal casting,²⁵ residential HVAC systems,²⁶ electrolysis to produce aluminum^{27,28,29} and chlorine,^{30,31} and seawater desalination,³² to name a few examples. There is also literature that considers generic processes with a more abstract focus.^{33,34} For an overview of the field, we refer to recent review articles.^{5,3,35} As mentioned before, the approaches presented assume given electricity prices, and their DR activities might suffer from the mismatch between grid assumptions and actually implemented demand depicted in Figure 1. If this mismatch has a significant impact, our cooperative approach⁸ might provide superior performance in congested grids. A vast amount of literature points out that distributed solution methods inherently minimize the shared information and explicitly specify the amount of shared information between the distributed participants.

For example, Allman and Zhang consider energy-intensive processes that participate not only in DR activities themselves, but also incentivize downstream processes to shift their demand accordingly.³⁶

Distributed optimization is also used to coordinate DC power networks with fixed electric loads and generation plants using natural gas,³⁷ electric vehicle charging stations and electric vehicle aggregators,³⁸ different regions in large-scale conventional AC OPF problems,³⁹ and AC microgrids and battery swapping stations.⁴⁰ These approaches use Lagrangian-relaxation-based techniques such as subgradient methods or alternating direction method of multipliers⁴¹ because they model the participants under coordination using mixed-integer models or other formulations that induce a duality gap. Wenzel and Engell note that such market-like coordination methods suffer from slow convergence rates and propose alternatives based on quadratic approximation models.⁴² However, the dynamic closed-loop behavior of energy-intensive chemical processes that we consider can be approximated with (low dimensional) linear state-space models.^{8,43,44} This then allows the use of Benders decomposition (BD),⁴⁵ which relies on models with zero duality gap.

BD was initially introduced to exploit block structure in the constraint matrix of mixed integer linear programs (MILPs) and enable faster solution thereof. We propose to use BD to protect confidential information embedded in the subproblem models, an idea already discussed by Li et al.⁴⁶ It is important to emphasize that such use of BD is not intended to speed up computations. Rather, the time to compute the solution is likely to increase compared to the integrated model, but the decoupled formulation allows to find a solution by iteratively refining the representation of feasible power profiles. A comprehensive review covering both applications and theoretical developments of BD is provided by Rahmaniani et al.⁴⁷

4 | SOLUTION STRATEGY: COOPERATIVE OPF WHILE PROTECTING PROCESS INFORMATION

BD is suitable to decompose the integrated formulation of cooperative OPF problems: the concepts of master stage and subproblem stage correspond to the grid component and the process component of the integrated problem. Based on the communication scheme between the master stage and the subproblem stage of BD, we develop an algorithm to compute cooperative OPF solutions while only communicating information about the power demand profiles of cooperating processes. To include control over the power profile of cooperating end-users, we split the $P_{i,t}^{\text{load}}$ that appear as fixed values in (1b) into $P_{i,t}^{\text{load,fix}}$ and $P_{i,t}^{\text{load,coop}}$. While $P_{i,t}^{\text{load,fix}}$ remain fixed values that represent non-cooperating loads on bus i , $P_{i,t}^{\text{load,coop}}$ are new decision variables representing the power profile of a cooperating load on bus i . In the next section, we form process subproblems from state-space representations of the closed-loop dynamic process behavior. These subproblems are solved at the cooperating end-user's site. From them, we can derive conditions that the master variables $P_{i,t}^{\text{load,coop}}$ have to satisfy for feasible operation of the cooperating process located on

bus i . Afterward, we describe iteratively adding these conditions to the master problem.

4.1 | The subproblems

We use linear input–output state-space models in discrete time for the critical variables relevant to power demand of an industrial chemical process that is connected to the grid.⁸ This description of the process behavior has the following form:

$$\mathbf{x}_{t+1} = \mathbf{A}\mathbf{x}_t + \mathbf{B} \begin{pmatrix} p_t \\ \mathbf{u}_t \end{pmatrix}, \quad \forall t \in \{1, \dots, H-1\} \quad (2)$$

where $\mathbf{x}_t \in \mathbb{R}^{n_x}$ and $\mathbf{x} \in \mathbb{R}^{n_x \times H}$ represent the n_x state variables relevant to power demand at one, respectively, all time steps. An example for such a state is the amount of stored mass of a product or intermediate. Explicitly sharing terms with \mathbf{x}_t is undesired, as it reveals confidential information, such as process production capacity and energy efficiency. $\mathbf{p} \in \mathbb{R}^H$ represents the power profile, consisting of the power demand p_t at all time steps t . Finally, $\mathbf{u}_t \in \mathbb{R}^{n_u}$ or $\mathbf{u} \in \mathbb{R}^{n_u \times H}$ are n_u other inputs to the system at one, respectively all-time steps which in contrast to \mathbf{p} should not be shared explicitly. \mathbf{A} denotes the state matrix, \mathbf{B} denotes the input matrix. They can be regressed from data either collected from the process, or generated from fundamental physics-based models of the chemical process. Besides simplicity of the development, other advantages of such a process description are the low computational complexity of solving optimization problems with linear models, and that the behavior of the process is still well predicted.⁸

We complete the model of the chemical process with linear constraints that represent operational requirements such as product demand, product quality, and safety constraints and physical bounds on \mathbf{x} , \mathbf{p} , and \mathbf{u} :

$$\mathbf{M}\mathbf{x}_t \geq \mathbf{b}, \quad \forall t \in \{1, \dots, H\} \quad (3)$$

$$\mathbf{x}_t \in [\mathbf{x}^{lb}, \mathbf{x}^{ub}], \quad \forall t \in \{1, \dots, H\} \quad (4)$$

$$p_t \in [p^{lb}, p^{ub}], \quad \forall t \in \{1, \dots, H\} \quad (5)$$

$$\mathbf{u}_t \in [\mathbf{u}^{lb}, \mathbf{u}^{ub}], \quad \forall t \in \{1, \dots, H\} \quad (6)$$

The model (2)–(6) describes feasible operating schedules of the chemical process it represents. Thus, we could set the values of \mathbf{p} to values of a solution candidate proposed by the master variables $\mathbf{p}_{i,t}^{\text{load,coop}}$. Because the master problem only includes an outer approximation of the projection of (2)–(6) to the space of $\mathbf{p}_{i,t}^{\text{load,coop}}$, a candidate solution will likely render the subproblem infeasible. Then, in the decoupled cooperative OPF approach, we must to generate inequality constraints formulated in the variables $\mathbf{p}_{i,t}^{\text{load,coop}}$. These “feasibility cuts” can be derived from an unbounded ray of the dual problem corresponding to the primal infeasible subproblem.⁴⁵ However, it is theoretically possible that the dual problem corresponding to an infeasible primal problem is also infeasible. In practice, this issue can be

circumvented with a feasible formulation,⁴⁸ using slacks that penalize infeasible values of $\mathbf{p}_{i,t}^{\text{load,coop}}$. Therefore, the following subproblem effectively minimizes the distance between the power profile suggested by the master solution for the $\mathbf{p}_{i,t}^{\text{load,coop}}$ and a feasible power profile \mathbf{p} :

$$\min_{\mathbf{x}, \mathbf{u}, \mathbf{p}, \mathbf{s}^+, \mathbf{s}^-} \sum_{t=1}^H s_t^+ + s_t^- \quad (7a)$$

s.t.

$$(2)–(6)$$

$$\mathbf{s}^+, \mathbf{s}^- \geq \mathbf{0} \quad (7b)$$

$$p_t = \mathbf{p}_{i,t}^{\text{load,coop}} + s_t^+ - s_t^-, \quad \forall t \in \{1, \dots, H\} \quad (7c)$$

where feasible suggestions $\mathbf{p}_{i,t}^{\text{load,coop}}$ can be identified by an optimal subproblem objective of zero. Each cooperating process is represented by one subproblem.

The cuts generated by problem (7) have the following form⁴⁵:

$$\sum_{t=1}^H \lambda_t^{\text{coup}} \cdot \mathbf{p}_{i,t}^{\text{load,coop}} \geq \lambda^\top \mathbf{r} \quad (8)$$

where λ denotes the dual variables corresponding to problem (7), λ_t^{coup} are its entries corresponding to the t^{th} equation of the form (7c), which couples p_t and $\mathbf{p}_{i,t}^{\text{load,coop}}$. The vector \mathbf{r} gathers the right-hand sides of problem (7) in standard linear programming (LP) form, that is, all terms that do not contain any decision variables of (7), except for the $\mathbf{p}_{i,t}^{\text{load,coop}}$ because these values are variables of the master problem.⁴⁸

4.2 | The master problem

We derive the master problem from problem (1). We retain the objective and most of the constraints of (1). As already mentioned, we split the $\mathbf{p}_{i,t}^{\text{load}}$ in (1b) into $\mathbf{p}_{i,t}^{\text{load,fix}}$ and $\mathbf{p}_{i,t}^{\text{load,coop}}$. Also, we copy box constraints for $\mathbf{p}_{i,t}^{\text{load,coop}}$ from (5) into the master problem as an initial outer approximation of the feasible region of power profiles \mathbf{p} in (2)–(6). We refine this outer approximation by adding a BD-type cut of the form (8) in each iteration of our decoupled solution algorithm. The master problem is:

$$\min_{\mathbf{p}^{\text{gen}}, \mathbf{T}, \theta, \mathbf{p}^{\text{load,coop}}} \sum_{i \in \Omega_{\text{Bus}}} \sum_{t=1}^H F_i(\mathbf{p}_{i,t}^{\text{gen}}) \quad (9a)$$

s.t.

$$\mathbf{p}_{i,t}^{\text{gen}} - \left(\mathbf{p}_{i,t}^{\text{load,fix}} + \mathbf{p}_{i,t}^{\text{load,coop}} \right) = \sum_{j \in \Omega_i^{\text{d}}} T_{(ij),t}, \quad \forall i \in \Omega_{\text{Bus}}, t \in \{1, \dots, H\}, \quad (9b)$$

$$(1c) - (1i), \quad \forall t \in \{1, \dots, H\},$$

$$\mathbf{p}_{i,t}^{\text{load,coop}} \in [p^{lb}, p^{ub}], \quad \forall i \in \Omega_{\text{Bus}}, \quad \forall t \in \{1, \dots, H\}, \quad (9c)$$

$$\text{BD - Cuts (8)}. \quad (9d)$$

4.3 | A decoupled solution strategy

In each iteration, the solution of the master problem provides power profiles that minimize the power flow cost, given the current outer approximation of the feasible set of power profiles. Our algorithm terminates if the master problem suggests feasible power profiles for all cooperating end-users, meaning that power profiles which are both cost-optimal and feasible were identified. Otherwise, for each infeasible power profile suggestion, the corresponding subproblem will add a cut to the master problem. In the next iteration, the previously proposed power profile will be infeasible in the master problem, so a new suggestion will be found. We sketch the communication scheme between grid and cooperating process in Figure 2.

An advanced basis start allows to solve the individual linear problems efficiently. Convergence of the proposed algorithm follows directly from Reference 45. Consequently, the integrated solution can be recovered with finitely many iterations.

Equation (8) shows that only dual coefficients corresponding to coupling equations and the scalar product $\lambda^T r$ are shared with the grid. These cuts do not allow to reconstruct or “reverse engineer” entries or dimensions of A , B , M , or b , nor the solution values of the internal variables x , u or dual variables from λ that do not correspond to (7c).

Any communication between the grid (master problem) and participating electricity-intensive entities (subproblems) consists of exchanging information only in the space of power profiles. Besides the cuts, the master problem is only informed about the box constraints (5) to derive

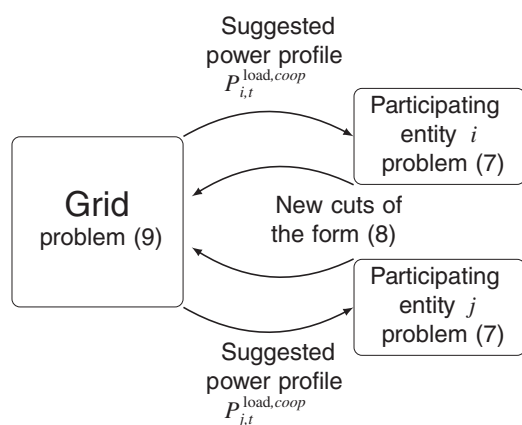


FIGURE 2 At the start of the algorithm, box constraints for the power profile variables of the cooperating plant, $p_{i,t}^{load,coop}$ are available at the grid level. At every iteration, problem (9) is solved, resulting in a new power profile for the plant, suggested by the grid. Because this suggestion only reflects an outer approximation of the feasible region of power profiles, the suggestion will likely be infeasible. Then, the entity i generates a cut that by construction cuts off the previous suggestion from the outer approximation of the feasible region of power profiles in the grid model. Iteratively, the outer approximation is refined, so when the grid eventually suggests a feasible power profile to all entities, the algorithm terminates. The feasible power profile belongs to a solution of the integrated problem formulation, which is recovered without revealing process details to the grid

(9c). For the heuristic presented in the next section, the values of the slack variables s^+ and s^- from the subproblems (7) will also be shared with the grid. They represent the difference between the profile suggested by the $p_{i,t}^{load,coop}$ and a feasible power profile. Thus, this is also an information exchange in the space of power profiles.

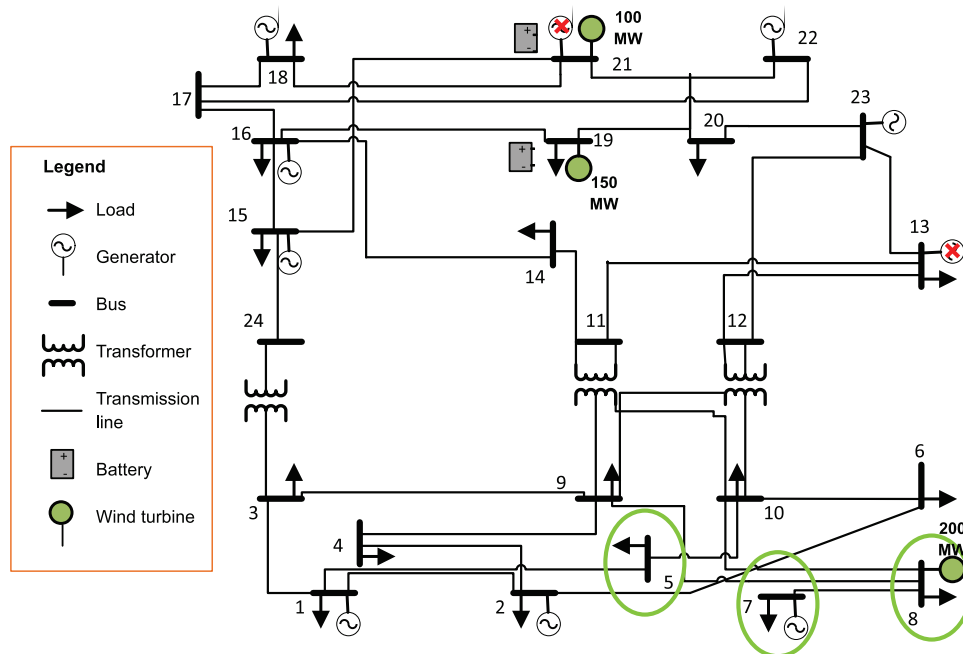
Malicious use of the information shared in this cooperation allows only to derive a very accurate description of the projection of the feasible set of the process model to the space of power profiles. However, any process regularly participating in any kind of price-based DR would reveal such information as well. Also, we anticipate that attempts to generate this projection in a detailed way would be noticed by cooperating end-users because a huge number of iterations would be required to even converge the BD for a single objective direction of the master problem. As we will describe, our decoupling strategy terminates with close-to-optimal solutions after a few hundred iterations, far before BD converges. Since malicious exploration of the whole projection of the feasible set of the process to the space of power profiles requires the convergence for many different master objective directions, the number of iterations required for such intents will exceed the normal number of iterations by several orders of magnitude.

4.4 | A heuristic for acceptably good solutions

In practice, we experienced numerical difficulties when the subproblem objectives are approaching zero, that is, the power profiles suggested by the master stage are nearly feasible. In particular, the distance between cuts generated by the subproblems and the previous suggestion is below the feasibility tolerance, so the LP-solver of the master stage fails to compute a new solution. To circumvent these numerical issues, we propose to terminate the algorithm with a nearly optimal solution at an acceptable optimality gap. As a beneficial side-effect, such a termination also saves substantial computational effort without compromising the economically favorable effects of the cooperative OPF solution, as we illustrate in Figure 6.

To compute an optimality gap, an upper bound and a lower bound are needed for the cooperative OPF objective, which reflects the generation and transmission cost of the grid. Since the master problem uses an outer approximation of the true feasible region of power profiles of cooperating plants, every solution of the master problem is a valid lower bound for the cooperative OPF objective. Furthermore, this bound is monotonically increasing as we add new cuts to refine the outer approximation of feasible power profiles. An upper bound for the cooperative OPF objective is given by the generation and transmission cost when the power profiles of all cooperating processes are fixed to any feasible profile. A feasible power profile is computed in every subproblem iteration by construction of (7c) by adding or subtracting necessary slack variables to the master suggestion $p_{i,t}^{load,coop}$. However, to obtain a sharp upper bound, it is necessary to optimize the remaining grid decision variables, that is, the solution of a conventional OPF is required, at a non-negligible computational cost. During our preliminary studies, we found that the sum of all

FIGURE 3 Modified IEEE 24 bus reliability test grid.¹¹ We place concentrated cooperating loads of 71 MW on bus 7 in the first case study and on bus 5 in the second case study, and distributed cooperating load along buses 5, 7, and 8 in the third case study. In our congested grid model, we decrease the total generation capacity of the grid by 24%. We model this circumstance as a complete failure of the largest generator which is located on bus 13 and by reducing the generator capacity of the second-largest generator, which is located on bus 21, by 225 MW



subproblem objectives—which is available in each iteration without additional effort—is almost proportional to the optimality gap. We thus derive the following heuristic to efficiently terminate the decoupled cooperative OPF problem with an acceptable optimality gap: An upper bound for the cooperative OPF objective is only computed when the sum of all subproblem objectives falls below a threshold τ . If the obtained optimality gap ω is greater than the acceptable optimality gap ω_{acc} , we reduce the threshold τ by a factor of ω/ω_{acc} . This procedure avoids the need to solve many conventional OPF problems, but still detects acceptable solutions reliably. Further implementation details can be inspected in our open-source code at <http://permalink.avt.rwth-aachen.de/?id=620241>.

5 | CASE STUDY

With our case study, we seek to reproduce the results from the case study in our previous work using the proposed decoupled formulation of cooperative OPF.⁸ We use the modified IEEE 24 bus reliability test grid proposed by Soroudi.¹¹ Figure 3 visualizes this transmission grid; it contains 12 generators and 17 load locations. Electrical batteries, wind farms and generation and demand pattern for wind turbines and connected loads are included as described in Reference 11.

In the subproblems, the electric load of the cooperating end-users is modeled with linear state-space dynamic process models. Here, we consider a chlor-alkali process. Its model of the form (2)–(6) reliably predicts its behavior.⁸ The chlor-alkali process comprises numerous electrolyzers running in parallel. Because the operational characteristics of the process are independent of the number of electrolyzers, the model can be arbitrarily scaled to different numbers of electrolyzers and thus total process loads. If not specified otherwise, we use a process with a nominal power draw of 71 MW, which

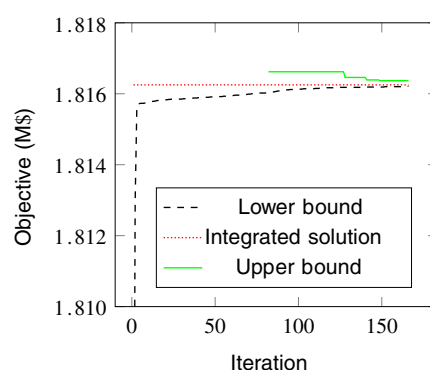


FIGURE 4 Convergence of the decoupled algorithm for 71 MW cooperating load on bus 5 in a congested grid. The dashed black line is the master problem objective, and the solid green line indicates the objective value of the best feasible solution identified. Note that the computation of the upper bound requires the solution of a non-cooperative optimal power flow (OPF) problem. In this case study, the first upper bound is computed in iteration 82, where the green line starts. The objective value of the optimal integrated solution is shown by the dotted red line

corresponds to 2.5% of the total load in the grid. Following Reference 8, we examine our algorithm on two cases of cooperating loads concentrated on a single bus and one case of cooperating load distributed along the grid. We place the concentrated load on bus 7 in the first case study and bus 5 in the second. The former is a bus with on-site generation; the latter is a load-only bus. For the distributed load, we choose buses 5, 7, and 8 in the third case study.

The master problem with one cooperating load has a size of 11,617 rows plus one row per iteratively added cut, 12,865 columns, and 38,567 nonzero matrix entries. For each additional bus with cooperating loads, 96 columns and 96 nonzero matrix entries are

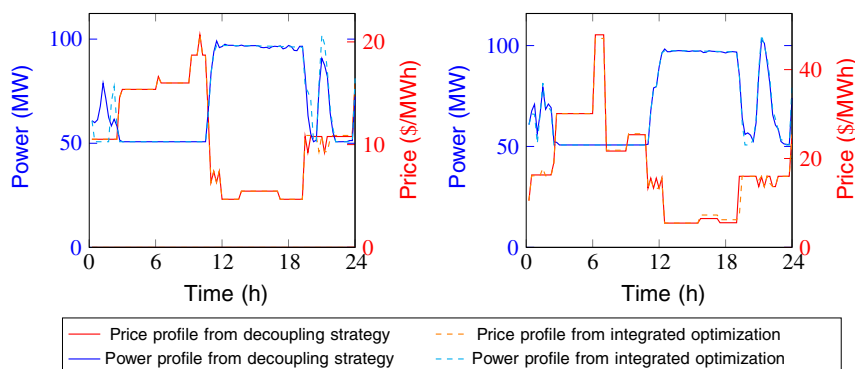


FIGURE 5 Power profiles and price profiles obtained from the decoupling strategy and model-sharing integrated optimization take a similar course. We place a cooperating end-user with the nominal power draw of 71 MW on bus 5. The left plot shows the results for normal grid conditions, the right plot shows results in a congested grid

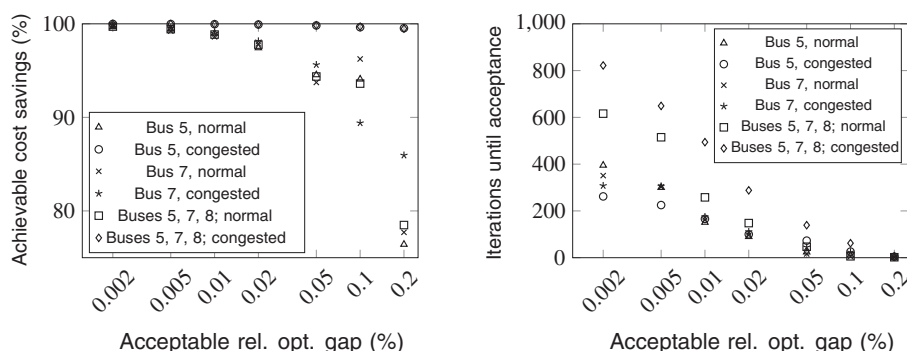


FIGURE 6 The acceptable gap can be loosened or tightened to balance the number of iterations and the closeness of the obtained solution to the integrated solution. The realized cost savings converge toward 100% of the achievable savings with tightening tolerances as shown on the left. Simultaneously, tighter tolerances require more iterations as shown on the right. These two trends motivated a default optimality gap choice of 0.01%

added. Each subproblem has 14,018 rows, 14,209 columns, and 50,394 nonzero matrix entries.

We study all setups in both congested and noncongested grids. We model congestion by removing the generator on bus 13 completely and reducing the generation capacity of the generator on bus 21 by 225 MW. This corresponds to a decrease of 24% of the total generation capacity originally available to the grid. Congestion always occurs in the transmission line connecting bus 7 to bus 8 in all case studies we carried out.

We implemented our algorithm in C++, using Gurobi 9.1.1 as the linear program solver. Gurobi reads our models as *.lp-files and allows direct access to the models to add cuts iteratively. Then, a warm start can be used in the next iteration to solve the LPs again. We conduct all calculations on a server with two Intel(R) Xeon(R) Gold 5117 CPUs at 2.00 GHz and 320 GB RAM. We provide our maintained implementation of the algorithm as open-source code in the repository linked above.

6 | RESULTS AND DISCUSSION

6.1 | Obtaining nearly optimal cooperative solutions

The decoupling strategy achieves nearly the same cost reductions for the grid and the cooperating consumers as the integrated solution that relies on fully shared process models. Figure 4 shows the convergence of the master problem objective function values, which is a monotonic lower bound on the optimal integrated solution objective,

and the best feasible solution found, which is an upper bound on the optimal integrated solution objective over the course of the iterations for the congested case with a 71 MW cooperating load on bus 5.

Table 1 compares the cost savings computed with both strategies for setups with the cooperating load concentrated on a single bus. Table 2 shows those results for a setup in which the cooperating load is distributed along the grid on buses 5, 7, and 8. For both strategies, we report cost savings relative to nominal operation, where the power consumption of the process is constant at all times. This is a reasonable benchmark for the grid-level economics. For the electricity cost of the process, we report the savings achieved by our cooperation scheme and achievable by DR activities of the process. For the DR activities, we use the electricity prices provided by the grid-level computations that assumed nominal process operation. As visualized in Figure 1, we remark that prices and corresponding DR power profiles are not guaranteed to ever reach a consensus regarding the underlying assumptions. Both Tables 1 and 2 show that the decoupled solution achieves nearly the same cost savings as the integrated OPF. As we already reported in our previous work,⁸ cooperation of the load located on bus 7 is less effective than cooperation of other buses because the transmission line connecting buses 7 and 8 is congested in the congested setup. This effect can again be seen in Table 1, where the cost reductions in a congested grid are a lot higher when the cooperating load is placed on bus 5 instead of bus 7. As explained in our previous work,⁸ the flexible cooperation of 2.5% of grid load reduces generation cost by significantly reducing the generation prices, that is, shifting more generation duty to cheap generators if possible.

The decoupled solution also results in power profiles and price profiles that closely follow their counterparts from the integrated

TABLE 1 Cooperative cost reductions with flexible load on a single bus for integrated and decoupled optimization

Cooperative load location, scenario	OPF cost reduction vs. nominal operation		Process energy cost reduction by DR to grid prices	Process energy cost reduction vs. nominal operation	
	Integrated	Decoupled		Integrated	Decoupled
Bus 5, normal	0.514%	0.508%	13.5%	12.5%	12.4%
Bus 7, normal	0.514%	0.507%	13.5%	12.5%	12.3%
Bus 5, congested	15.2%	15.2%	21.5%	48.7%	48.6%
Bus 7, congested	0.679%	0.672%	15.3%	12.8%	13.5%

TABLE 2 Cooperative cost reductions with distributed flexible load for integrated and decoupled optimization

Scenario	OPF cost reduction vs. nominal operation		Location of coop. load	Process energy cost reduction by DR to grid prices	Process energy cost reduction vs. nominal operation	
	Integrated	Decoupled			Integrated	Decoupled
Normal	0.514%	0.508%	Bus 5	13.5%	12.5%	12.4%
			Bus 7	13.5%	12.5%	12.4%
			Bus 8	13.5%	12.5%	12.2%
Congested	14.8%	14.8%	Bus 5	21.6%	46.6%	46.5%
			Bus 7	15.3%	12.7%	12.5%
			Bus 8	21.6%	46.6%	46.3%

model. We visualize this in Figure 5 for the setup with flexible load concentrated on bus 5, as an example. The close match between profiles computed from the decoupling strategy and integrated optimization is also present for the other setups we investigated, but we omit their visualizations in the interest of brevity. We note that price profiles and power profiles differ only because the iterative procedure stops with an acceptable optimality gap. In theory, iterating until convergence leads to concordant solutions—assuming a unique optimal solution, that is, no degeneracy.

6.2 | Trade-off between acceptable optimality gap and computational effort

The optimality gap ω that the user considers acceptable influences the computational effort necessary to compute an acceptable solution and how close such a solution is to the integrated solution. The decoupling strategy realizes a lot of the cost savings that cooperative formulation can achieve, even with relatively loose acceptable gaps, as illustrated in Figure 6. Even with the loosest acceptable optimality gap of 0.2%, our decoupling strategy accomplishes over 75% of the achievable cost savings relative to nominal operation in all setups. Reducing the acceptable threshold to 0.01%, over 98.5% of the achievable cost savings were obtained in all instances considered.

Figure 6 shows the number of iterations required until an acceptable solution is found. A loose optimality gap requires only few

iterations, and our default acceptable optimality gap of 0.01% requires a few hundred iterations; for even tighter optimality gaps, the iterations required increase further, while the marginal economic benefit diminishes.

The computational runtime, as visualized in Figure 7, confirms the trend toward increasing computational effort for very tight optimality gaps. The computations were not performed on an otherwise idle machine, so the exact numbers might not be reproducible, but the overall trend is clear. The relative share of the computational time spent in the subproblem stage decreases as the number of cooperating end-users increases. This is because the size of the subproblems is fixed and they are solved in parallel. In contrast, the master problem is hard to parallelize, and it contains more variables and cuts as the number of cooperating end-users increases. Figure 7 also confirms that the adaptive threshold selection for the feasible point assessment works well in practice. This stage requires by far the least computational time. Considering the alternative of having to iterate until convergence to the integrated solution, this computational effort is well allocated.

6.3 | Computational effort for multiple buses with flexible load

In Figure 7, we already saw an important limitation of the proposed decoupled problem formulation: The computational effort for finding an acceptable solution for the decoupled problem increases

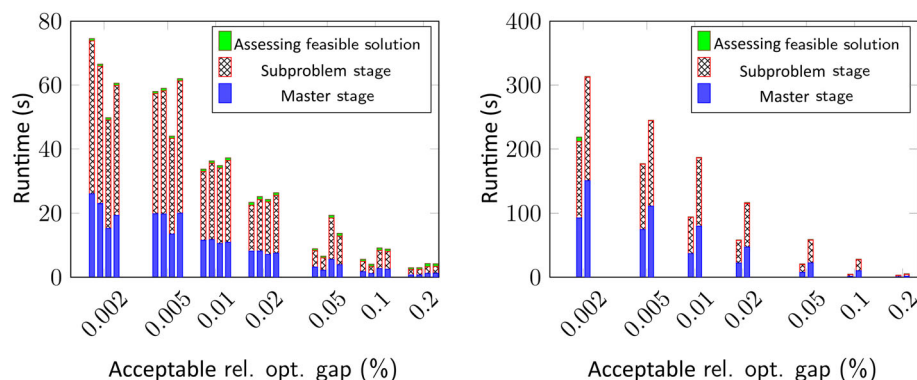


FIGURE 7 Visualization of runtimes of problem stages until convergence to an acceptable gap. Tighter acceptable gaps require longer runtime, and the actual runtimes are problem-dependent. The left figure shows cases with 71 MW cooperating load concentrated on one bus for each acceptable gap. From left to right, the load is placed on: bus 5 in normal grid, bus 5 in congested grid, bus 7 in normal grid, and bus 7 in congested grid. The right figure shows results for cases with 71 MW cooperating load distributed on buses 5, 7, and 8. For each acceptable gap, the left/right bars show results of the normal grid/congested grid setup. The master stage and the subproblem stage require the majority of computation time, with the relative share of the master stage increasing with more buses with cooperating load as multiple subproblems run in parallel. Assessing the optimality gap of a feasible solution to terminate the algorithm has negligible computational effort with our heuristic stopping criterion

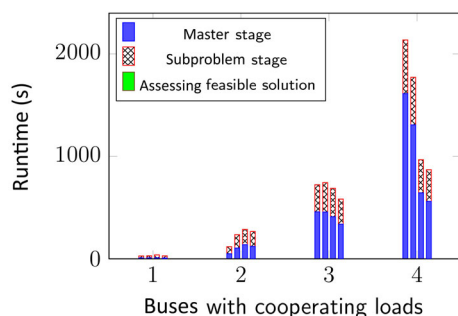


FIGURE 8 Scaling behavior of the decoupled problem regarding multiple cooperating end-users: We show four cases for each number of buses with cooperating loads. From left to right, these are: A in normal grid, B in normal grid, A in congested grid, and B in congested grid. The computation time is quickly increasing with increasing cooperative bus count. On the one hand, the increase is driven by the master problem stage, which becomes more complex when more processes need to be represented and increases its relative share of the total runtime. Furthermore, the master problem stage is hard to parallelize. On the other hand, finding the optimal solution with multiple buses with cooperating loads requires more iterations, which increases the total computational effort. Once again, the computational effort for assessing if feasible solutions are acceptable is negligible

dramatically when the number of buses with cooperating load increases. To study this effect further, we present two scenarios in which we increase the number of buses with cooperating end-users. For scenario A, we start with bus 5 and add buses 10, 9, and 19 in that order. Similarly, we define scenario B to start with bus 7, successively completed by buses 6, 10, and 16. On each bus, we model the cooperative load to be 50% of the total bus load of that bus. We always use our model for the chlor-alkali process as the subproblem and run the

computations in normal and congested grid setups. Our results are visualized in Figure 8.

The computational effort for solving these problems varies with the case definition, that is, the selection of buses with cooperating end-users and whether or not the grid is in a congested state. When more buses have a cooperating load, the master problem becomes larger as it needs to represent the power profiles of more processes with variables, box constraints, and iteratively generated cutting planes. We remark that the computational effort scaling corresponds only to the number of buses with cooperating load, not the amount of flexible cooperating load in the grid. Therefore, the general trend of increasing computational effort with an increasing number of buses with cooperating end-users is intuitive. However, the significant increase shown in Figure 8 is surprising and calls for further research attention. Besides more sophisticated algorithmic developments, a practical compromise to solve large problems with many cooperating end-users could be to loosen the acceptable relative optimality gap or terminate after a fixed number of iterations with the best found solution.

7 | CONCLUSIONS AND FUTURE WORK

We solve cooperative optimal power flow (OPF) problems by sharing limited information between the grid operator and participating loads by using a Benders decomposition (BD)-inspired communication scheme between the master and subproblem stages. Our decoupling method achieves significant fractions of the attainable cost savings of the cooperative formulation of the OPF problem in an acceptable number of iterations and computational time. By adjusting the acceptable optimality gap, it is possible to trade accuracy for computational effort and vice versa.

Future research should consider improvements in the scaling behavior of the method regarding the number of buses with cooperating end-users. Also, the approach extends to more complicated models, for example, mixed-integer master problems. With a generalized BD,^{49,50} more general process models can be used to represent processes (participating loads) that cannot be described accurately with linear models.

ACKNOWLEDGMENTS

This work was funded by the Deutsche Forschungsgemeinschaft (DFG, German Research Foundation) - 33849990/GRK2379 (IRTG Modern Inverse Problems). Partial financial support for Michael Baldea from the National Science Foundation (NSF) through the CAREER Award 1454433 is acknowledged with gratitude.

AUTHOR CONTRIBUTION

Tim Varelmann: Formal analysis (lead), Investigation (equal), Methodology (equal), Software (equal), Visualization (equal), Writing-original draft (equal); **Joannah Otashu:** Methodology (supporting), Software (supporting); **Kyeongjun Seo:** Investigation (supporting), Methodology (supporting), Software (supporting); **Adrian Lipow:** Investigation (supporting); **Alexander Mitsos:** Funding acquisition (supporting), Supervision (equal), Writing-review & editing (supporting); **Michael Baldea:** Conceptualization (lead), Funding acquisition (lead), Investigation (supporting), Methodology (supporting), Project administration (lead), Supervision (equal), Writing-review & editing (Lead).

DATA AVAILABILITY STATEMENT

Data sharing is not applicable to this article as no new data were created or analyzed in this study.

ORCID

Tim Varelmann  <https://orcid.org/0000-0002-9487-1688>

Adrian W. Lipow  <https://orcid.org/0000-0002-5860-5323>

Alexander Mitsos  <https://orcid.org/0000-0003-0335-6566>

Michael Baldea  <https://orcid.org/0000-0001-6400-0315>

REFERENCES

1. Fang X, Misra S, Xue G, Yang D. Smart grid – the new and improved power grid: a survey. *IEEE Commun Surv Tutor*. 2012;14(4):944-980.
2. Gungor VC, Sahin D, Kocak T, et al. A survey on smart grid potential applications and communication requirements. *IEEE Trans Ind Inf*. 2013;9(1):28-42.
3. Zhang Q, Grossmann IE. Planning and scheduling for industrial demand side management: advances and challenges. *Alternative Energy Sources and Technologies*. Springer; 2016:383-414.
4. Baldea M. *Employing Chemical Processes as Grid-Level Energy Storage Devices*. Springer International Publishing; 2017:247-271.
5. Palensky P, Dietrich D. Demand side management: demand response, intelligent energy systems, and smart loads. *IEEE Trans Ind Inf*. 2011; 7(3):381-388.
6. Samad T, Kiliccote S. Smart grid technologies and applications for the industrial sector. *Comput Chem Eng*. 2012;47:76-84. FOCAP 2012.
7. Mirakhorli A, Dong B. Model predictive control for building loads connected with a residential distribution grid. *Appl Energy*. 2018;230: 627-642.
8. Otashu JI, Seo K, Baldea M. Cooperative optimal power flow with flexible chemical process loads. *AIChE J*. 2021;67:e17159.
9. Bacher R. Power system models, objectives and constraints in optimal power flow calculations. *Optimization in Planning and Operation of Electric Power Systems*. Springer; 1993:217-263.
10. Wood AJ, Wollenberg BF. *Power Generation, Operation, and Control*. John Wiley & Sons; 2013.
11. Soroudi A. *Power System Optimization Modeling in GAMS*. Vol 78. Springer; 2017.
12. McAuliffe P, Rosenfeld A. *Response of Residential Customers to Critical Peak Pricing and Time-of-Use Rates during the Summer of 2003*. California Energy Commission; 2004.
13. Wu L. Impact of price-based demand response on market clearing and locational marginal prices. *IET Gener Transm Distrib*. 2013;7(10): 1087-1095.
14. Contreras J, Candiles O, De La Fuente JI, Gomez T. Auction design in day-ahead electricity markets. *IEEE Trans Power Syst*. 2001;16(1): 88-96.
15. Strbac G, Kirschen D. Assessing the competitiveness of demand-side bidding. *IEEE Trans Power Syst*. 1999;14(1):120-125.
16. Fioretto F, Van Hentenryck P. Constrained-based differential privacy: releasing optimal power flow benchmarks privately. *International Conference on the Integration of Constraint Programming, Artificial Intelligence, and Operations Research*. Springer; 2018:215-231.
17. Mak TW, Fioretto F, Shi L, Van Hentenryck P. Privacy-preserving power system obfuscation: a bilevel optimization approach. *IEEE Trans Power Syst*. 2019;35(2):1627-1637.
18. Anderson J, Zhou F, Low SH. Disaggregation for networked power systems. *2018 Power Systems Computation Conference (PSCC)*. IEEE; 2018:1-7.
19. Dwork C, Roth A. The algorithmic foundations of differential privacy. *Found Trends Theor Comput Sci*. 2014;9(3-4):211-407.
20. Ierapetritou M, Wu D, Vin J, Sweeney P, Chigirinskiy M. Cost minimization in an energy-intensive plant using mathematical programming approaches. *Ind Eng Chem Res*. 2002;41(21):5262-5277.
21. Zhang Q, Grossmann IE, Heuberger CF, Sundaramoorthy A, Pinto JM. Air separation with cryogenic energy storage: optimal scheduling considering electric energy and reserve markets. *AIChE J*. 2015;61(5): 1547-1558.
22. Caspari A, Offermanns C, Schäfer P, Mhamdi A, Mitsos A. A flexible air separation process: 2. Optimal operation using economic model predictive control. *AIChE J*. 2019;65(11):e16721.
23. Hadera H, Harjunkski I, Sand G, Grossmann IE, Engell S. Optimization of steel production scheduling with complex time-sensitive electricity cost. *Comput Chem Eng*. 2015;76:117-136.
24. Mitra S, Sun L, Grossmann IE. Optimal scheduling of industrial combined heat and power plants under time-sensitive electricity prices. *Energy*. 2013;54:194-211.
25. Ramin D, Spinelli S, Brusaferrri A. Demand-side management via optimal production scheduling in power-intensive industries: the case of metal casting process. *Appl Energy*. 2018;225:622-636.
26. Perez KX, Baldea M, Edgar TF. Integrated HVAC management and optimal scheduling of smart appliances for community peak load reduction. *Energy Buildings*. 2016;123:34-40.
27. Todd D, Caufield M, Helms B, et al. Providing reliability services through demand response: a preliminary evaluation of the demand response capabilities of Alcoa Inc. ORNL/TM-2008/233; 2008.
28. Zhang X, Hug G. Bidding strategy in energy and spinning reserve markets for aluminum smelters' demand response. *2015 IEEE Power & Energy Society Innovative Smart Grid Technologies Conference (ISGT)*. IEEE; 2015:1-5.
29. Schäfer P, Westerholt HG, Schweidtmann AM, Ilieva S, Mitsos A. Model-based bidding strategies on the primary balancing market for energy-intensive processes. *Comput Chem Eng*. 2019;120:4-14.

30. Roh K, Brée LC, Perrey K, Bulan A, Mitsos A. Optimal oversizing and operation of the switchable chlor-alkali electrolyzer for demand side management. *Computer Aided Chemical Engineering*. Vol 46. Elsevier; 2019:1771-1776.
31. Otashu JI, Baldea M. Scheduling chemical processes for frequency regulation. *Appl Energy*. 2020;260:114125.
32. Williams CM, Ghobeity A, Pak AJ, Mitsos A. Simultaneous optimization of size and short-term operation for an RO plant. *Desalination*. 2012;301:42-52.
33. Castro PM, Harjunkoski I, Grossmann IE. New continuous-time scheduling formulation for continuous plants under variable electricity cost. *Ind Eng Chem Res*. 2009;48(14):6701-6714.
34. Schäfer P, Daun TM, Mitsos A. Do investments in flexibility enhance sustainability? A simulative study considering the German electricity sector. *AIChE J*. 2020;66(11):e17010.
35. Groppi D, Pfeifer A, Garcia DA, Krajačić G, Duić N. A review on energy storage and demand side management solutions in smart energy islands. *Renew Sustain Energy Rev*. 2021;135:110183.
36. Allman A, Zhang Q. Distributed cooperative industrial demand response. *J Process Control*. 2020;86:81-93.
37. Zhao B, Zlotnik A, Conejo AJ, Sioshansi R, Rudkevich AM. Shadow price-based coordination of natural gas and electric power systems. *IEEE Trans Power Syst*. 2018;34(3):1942-1954.
38. Ding Z, Lu Y, Lai K, Yang M, Lee WJ. Optimal coordinated operation scheduling for electric vehicle aggregator and charging stations in an integrated electricity transportation system. *Int J Electr Power Energy Syst*. 2020;121:106040.
39. Erseghe T. Distributed optimal power flow using ADMM. *IEEE Trans Power Syst*. 2014;29(5):2370-2380.
40. Wang Y, Lai K, Chen F, Li Z, Hu C. Shadow price based co-ordination methods of microgrids and battery swapping stations. *Appl Energy*. 2019;253:113510.
41. Boyd S, Parikh N, Chu E. *Distributed Optimization and Statistical Learning via the Alternating Direction Method of Multipliers*. Now Publishers; 2011.
42. Wenzel S, Engell S. Coordination of coupled systems of systems with quadratic approximation. *IFAC-PapersOnLine*. 2019;52(3):132-137.
43. Tsay C, Baldea M. Integrating production scheduling and process control using latent variable dynamic models. *Control Eng Pract*. 2020;94:104201.
44. Otashu JI, Baldea M. Demand response-oriented dynamic modeling and operational optimization of membrane-based chlor-alkali plants. *Comput Chem Eng*. 2019;121:396-408.
45. Benders JF. Partitioning procedures for solving mixed-variables programming problems. *Numer Math*. 1962;4(1):238-252.
46. Li Y, Li Z, Wen F, Shahidehpour M. Privacy-preserving optimal dispatch for an integrated power distribution and natural gas system in networked energy hubs. *IEEE Trans Sustainable Energy*. 2018;10(4):2028-2038.
47. Rahmiani R, Crainic TG, Gendreau M, Rei W. The Benders decomposition algorithm: a literature review. *Eur J Oper Res*. 2017;259(3):801-817.
48. Birge JR, Louveaux F. *Introduction to Stochastic Programming*. Springer Science & Business Media; 2011.
49. Geoffrion AM. Generalized Benders decomposition. *J Optim Theory Appl*. 1972;10(4):237-260.
50. Li X, Sundaramoorthy A, Barton PI. *Nonconvex Generalized Benders Decomposition*. Springer; 2014:307-331.

How to cite this article: Varelmann T, Otashu JI, Seo K, Lipow AW, Mitsos A, Baldea M. A decoupling strategy for protecting sensitive process information in cooperative optimization of power flow. *AIChE J*. 2022;68(1):e17429. doi: 10.1002/aic.17429